

Endothelial Cell Response Under Hydrostatic Pressure Condition Mimicking Pressure Therapy

DAISUKE YOSHINO,¹ KAKERU SATO,^{2,4} and MASAOKI SATO³

¹Institute of Fluid Science, Tohoku University, 2-1-1 Katahira, Aoba, Sendai 980-8577, Japan; ²Graduate School of Engineering, Tohoku University, 6-6-01 Aramaki-Aoba, Aoba, Sendai 980-8579, Japan; ³Frontier Research Institute for Interdisciplinary Sciences, Tohoku University, 6-3 Aramaki-Aoba, Aoba, Sendai 980-8578, Japan; and ⁴Tokyo Gas Co., Ltd., 1-5-20 Kaigan, Minato-ku, Tokyo 105-8527, Japan

(Received 21 January 2015; accepted 13 March 2015; published online 20 March 2015)

Associate Editor Mian Long oversaw the review of this article.

Abstract—Chronic wounds increase the risk of infection and may lead to complications or disease. Although treatment techniques involving topical negative pressure have been used widely to promote wound healing, the relationship between promotion of wound healing and negative pressure remains unclear. In the present study, we studied the effects of hydrostatic pressure (HP) on endothelial cells (ECs) during pressure treatment. We examined the morphologic and functional responses of ECs to HP using an experimental system developed to apply both negative and positive pressure to ECs. Morphologic parameters such as aspect ratio, orientation angle, and tortuosity did not change after exposure to HP for up to 24 h. In contrast, application of HP led to significant changes in cell area and cell density, and the formation of intercellular gaps was observed as early as 3 h before the cell density reached its peak value. We also found HP progressed EC cycle, which remained at rest according to contact inhibition. Although there were some differences with respect to trends in changes in those parameters, positive and negative pressures had similar effects on ECs. Considering the results of this study, we conclude that exposure to HP enhances the proliferation of ECs.

Keywords—Positive pressure, Negative pressure, Endothelial morphology, Cellular area, Cell density, Cell cycle, Proliferation.

INTRODUCTION

Chronic wounds increase the risk of infection and may lead to complications or disease. Wounds are formed through rupture of the skin, bleeding, tissue destruction, and vascular rupture. The process of wound healing that begins following tissues damage has four phases: (i) blood clotting; (ii) inflammation;

(iii) fibroplasia and the formation of granulation tissue, during which connective tissues regenerate and the epidermis is restored in conjunction with angiogenesis of blood capillaries; and (iv) maturation. Synthesis of collagen by fibroblasts and capillary angiogenesis mediated by vascular endothelial cells (ECs) play particularly important roles during fibroplasia and the formation of granulation tissue.²⁴ Slight or less serious wounds tend to heal naturally. However, massive wounds that involve tissue necrosis or wounds resulting from surgical procedures are associated with increased risk of infection and subsequent complications or disease. Thus, safe and effective treatments for serious wounds are needed.

The application of topical negative pressure has received considerable attention recently as a potentially effective treatment for serious wounds and has been applied widely to promote wound healing.^{1,4,7,22} Application of negative pressure reportedly leads to improvement in various symptoms associated with wounds; for example, negative pressure may enhance elimination of exudate or infective materials, relieve edema, improve perfusion, and promote angiogenesis and the formation of granulation tissue.²¹ However, the detail mechanism underlying the promotion of wound healing through negative pressure are unclear though the clinical outcomes using the negative pressure treatment have already reported. Thus, due to the absence of authoritative evidence that negative pressure indeed promotes wound healing, further validation is necessary.²² In addition to the validation in a clinical site, it is necessary to elucidate effects of the pressure on wound healing at a cellular level.

Several studies examining the effects of hydrostatic pressure (HP) on cells have been reported. Negative pressure was shown to enhance the migration of epidermal cells.⁹ Negative pressure also enhances EC

Address correspondence to Daisuke Yoshino, Institute of Fluid Science, Tohoku University, 2-1-1 Katahira, Aoba, Sendai 980-8577, Japan. Electronic mail: yoshino.d@m.tohoku.ac.jp

proliferation and the three-dimensional migration of ECs into collagen gel.³ Positive pressure, on the other hand, promotes cell cycle progression in ECs and thus enhances their proliferation.¹⁹ However, understanding of how cells respond to HP remains limited, and thus there is not knowledge enough to clarify the mechanism through which pressure treatment promotes angiogenesis during wound healing. In this study, we focused on responses of ECs linked to angiogenesis, and adopted a two-dimensional assay under closed and pressured conditions mimicking the pressure treatment to find out important and fundamental results related to angiogenesis. With the goal of elucidating the details of the response of ECs to HP, we developed a novel experimental system to apply both positive and negative pressure to ECs and then used the system to characterize the morphological and functional responses of ECs.

MATERIALS AND METHODS

Development of a Novel Hydrostatic Pressure–Application System

Figure 1a shows a schematic of the newly developed experimental system for applying HP to cells. The system consists of a polycarbonate chamber, a pressure sensor (KEYENCE, GP-M001), two ball valves, a syringe, a silicone gasket for sealing, and a pair of jigs. All parts are joined with nylon couplings. Cell-culture dishes can be built directly into the system. The cell-culture dish is appressed to the polycarbonate chamber with the silicone gasket and the jigs. The system is completely closed, and the pressure can be stably maintained by closure of the two valves. Conditions of negative or positive pressure can be easily created by expanding or compressing the volume of culture medium, respectively, through the open of the valve in the side connecting to a syringe and the use of the syringe. The system produces only minimal changes in the concentrations of dissolved gasses.

Cell Culture

Human umbilical vein ECs (HUVECs; Cell Applications) from the fourth to eighth passages were used for the experiments in this study. HUVECs were cultured in 35-mm diameter glass-based dishes (Iwaki) that were pre-coated with 0.1% bovine gelatin (Sigma Aldrich). Cells were cultured in Medium 199 (Gibco) containing 20% heat-inactivated fetal bovine serum (FBS; Gibco), 10 $\mu\text{g/L}$ human basic fibroblast growth factor (bFGF; AUSTRAL Biologicals), and 0.1% penicillin/streptomycin (P/S; Gibco). Experiments

were conducted using Medium 199 containing 10% heat-inactivated FBS and 0.1% P/S (EM).

Exposure of HUVECs to HP

Confluent cultures of HUVECs were incubated in EM for 1 h after bFGF was washed out using EM. After incubation in EM, the cell culture dish was placed in the hydrostatic pressure–application system. The system was then filled with EM and HP was applied to the HUVECs. The system was maintained at 37 °C using a temperature-controlled incubator (AS ONE). We focused on cells exposed to HP of 0 (control), +50 mm Hg, and –50 mm Hg for 3, 6, 12, and 24 h. The trial for each time course existed independently of one another. The pressure value was determined by reference to a lower limit, which is actually used for the pressure treatment.^{11,23} Sample of ECs before treatment was defined as static condition.

Fluorescent Staining and Fluorescence Microscopy

After HP exposure, ECs were fixed with phosphate buffer containing 4% paraformaldehyde (Wako Pure Chemical Industries) for 15 min at room temperature. The fixed cells were then treated with 0.1% Triton X-100 (Wako Pure Chemical Industries) for 5 min for membrane permeabilization. After blocking with Block Ace (DS Pharma Biomedical) for 1 h, cells were incubated with anti-rabbit adherens junction protein (VE-cadherin) antibody (eBioscience) for 1.5 h and then incubated with secondary antibody conjugated with anti-rabbit Alexa Fluor 488 (Life Technologies) for 1 h. Cell nuclei were stained with DAPI (Life Technologies) for 5 min. The ECs were washed three times with Dulbecco's phosphate-buffered saline without Mg^{2+} and Ca^{2+} (PBS(–); Nissui Pharmaceutical) after each step. Stained ECs were observed using an inverted fluorescence microscope (Observer D1; Carl Zeiss).

Quantification of Morphologic Changes in ECs

To evaluate morphologic changes in ECs subjected to pressure treatment, we monitored the cellular aspect ratio, tortuosity, orientation angle, and area. The outlines of ECs selected at random were extracted from VE-cadherin fluorescence images, and then an ellipsoid corresponding to the shape of each cell was computed based on the extracted outline using ImageJ software (U.S. National Institutes of Health). The central coordinate, lengths of the major and minor axes, orientation angle, and perimeter of the ellipsoid equivalent to the EC were determined. The area and the perimeter of the cell could also be measured. Values for the parameters examined in this study were calculated based

on information obtained from the extracted outlines of the selected cells. The aspect ratio was defined as the ratio between lengths of the minor and major axes of the ellipsoid equivalent to the EC shape. The aspect ratio has a maximum value of 1 for a perfect circle, and it approaches zero for a highly elongated shape. Tortuosity was defined as the ratio between the cell perimeter and the perimeter of the equivalent ellipse of the cell.²⁰ The value for tortuosity increases from 1 as the shape of the cell becomes more tortuous, whereas a tortuosity value of 1 represents a cell shape corresponding to a perfect circle or ellipse. The orientation angle provides a measure of the angle between the major axis and a parallel line along the horizontal axis of the fluorescence image. We extracted 300 cells (100 cells per each sample) for each experimental condition. Cell density was defined as the number of ECs within a 100- μm square, and the number of cells was determined based on fluorescence images of nuclei captured within 430 μm \times 320 μm . Calculating the cell density, we used 30 images (10 images per each sample) for each condition. Only for the condition of +50 mmHg for 24 h, numbers of the extracted cells and images used for quantification are 400 cells (100 cells per each sample) and 40 images (10 images per each sample), respectively.

Cell Cycle Analysis

After exposure to HP, ECs were harvested from the dish by using 0.05% trypsin-EDTA (Gibco) and centrifuged after EDTA inactivation by EM. Then, ECs were rinsed twice with PBS(-) and fixed with 70% ice-cold ethanol. The sample was adjusted concentration of the cell solution 500 cells/ μL after washing again with PBS(-). DNA in the cell nucleus was stained with Guava Cell Cycle Reagent (Millipore) for 30 min, and then fluorescence intensity of 5000 cells, which is an effective measurement cell number, was measured. We conducted three trials per each experimental condition, and calculated the percentage of ECs existing in each phase of cell cycle. We used a flow cytometer (guava easyCyteTM 6HT; Millipore) for cell cycle analysis.

Data Quantification and Statistical Analysis

All values are shown as the mean \pm standard deviation (SD). Statistical significance between pressured and control conditions at the same time point was determined using analysis of variance or a two-tailed *t* test, with statistical significance set at $p < 0.01$ and $p < 0.001$, respectively. As all samples were independent of one another, the means and SDs were integrated, and a total mean and total SD for each

morphologic parameter were calculated using the following equations.⁸ The total mean value \bar{m}_t was expressed as

$$\bar{m}_t = \frac{\sum_{i=1}^k n_i \bar{m}_i}{n_t},$$

where \bar{m}_i represents the mean value of each sample, n_i represents the number of available data in each sample, n_t represents the total number of available data, i represents the sample number, and k represents the total number of samples, namely number of trials for each experimental condition. The total SD (σ_t) was obtained from

$$\sigma_t = \sqrt{\frac{\sum_{i=1}^k (n_i - 1)\sigma_i^2 + \sum_{i=1}^k (n_i \bar{m}_i - \bar{m}_t)^2}{n_t - 1}},$$

where σ_i represents the SD of each sample. For the analyses of aspect ratio, orientation angle, tortuosity, and cellular area, n_i was 100 cells and n_t was 300 cells for each condition or 400 cells only for the condition of +50 mmHg for 24 h. For analysis of cell density, on the other hand, n_i was 10 images and n_t was 30 images for each condition or 40 images only for the condition of +50 mmHg for 24 h

RESULTS

Performance of Hydrostatic Pressure–Application System

The performance of the system was evaluated by examining how well it maintained a pressure of 50 mmHg positive or negative HP at 37 °C over a period of 24 h, and the results are shown in Fig. 1b. Under conditions of both positive and negative pressure, the change in pressure remained within $\pm 6\%$. No changes in medium pH were observed. The theoretical rate of change in the concentration of a dissolved gas is approximately $\pm 7\%$ by calculating on the basis of modulus of volume change in the medium, and thus the partial pressure of oxygen under these experimental conditions is $21 \pm 1.47\%$.

Cell Orientation, Elongation, and Tortuosity

Fluorescence images of stained ECs were captured and used to quantitatively evaluate the morphologic changes resulting from pressure treatment, as shown in Fig. 2. Table 1 summarizes the aspect ratio, orientation angle, and tortuosity data for cells after exposure to HP. The aspect ratio was approximately 0.7 under all conditions examined. The tortuosity was approximately 1.1 under all conditions. Although significant differences

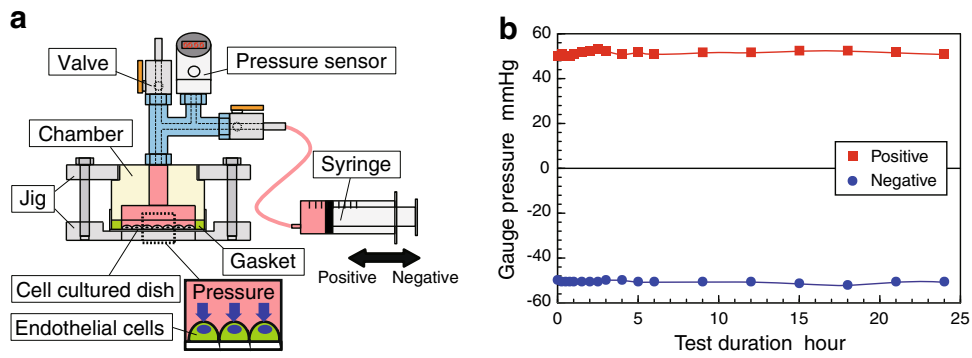


FIGURE 1. (a) Schematic diagram of the developed experimental system for applying HP to cells. (b) Monitoring of positive and negative pressure in the experimental system at 37 °C over a 24-h period.

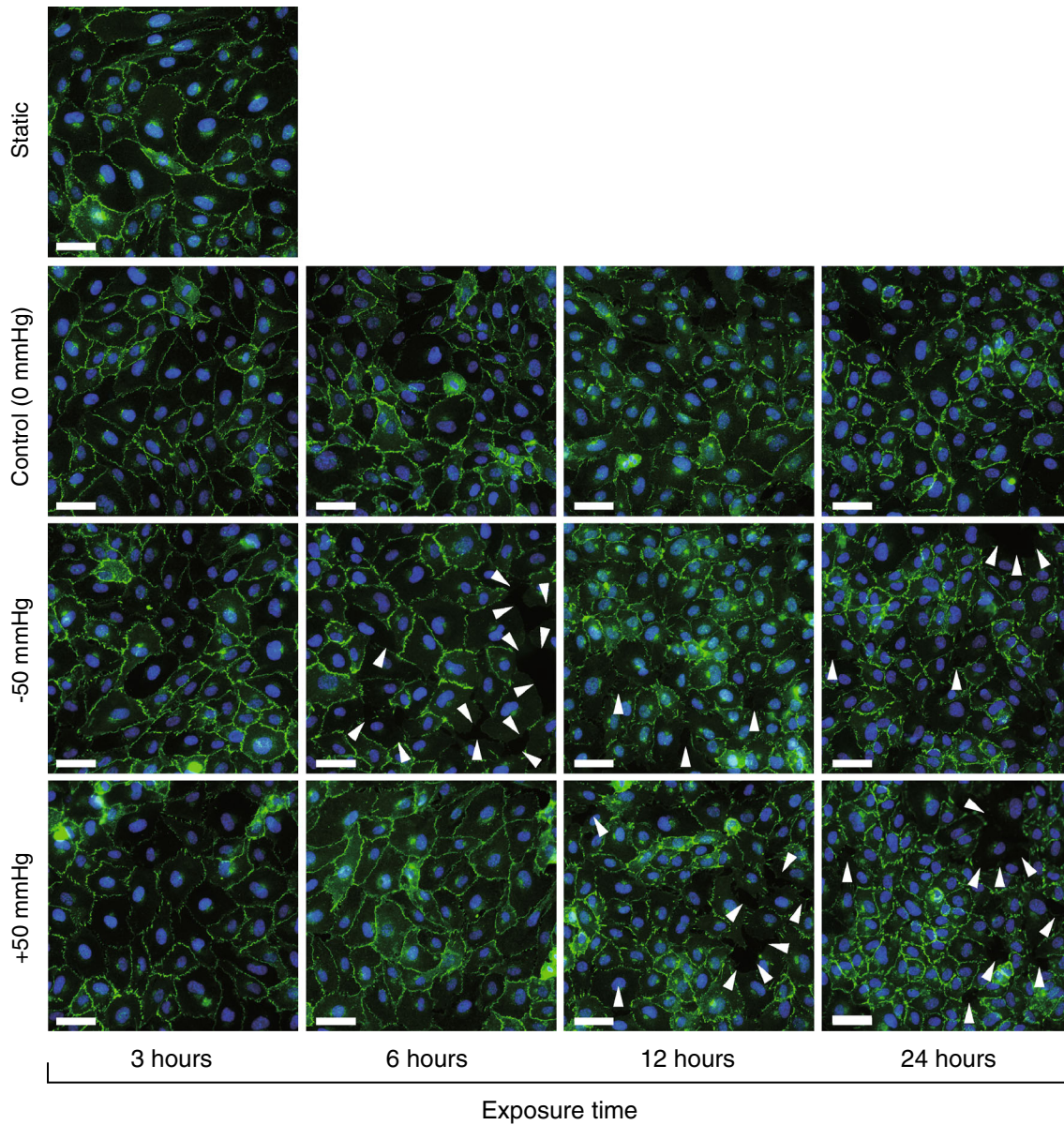


FIGURE 2. Representative fluorescence images of VE-cadherin and nuclei in ECs after exposure to HP. Green: VE-cadherin, blue: nuclei. The scale bars in all images represent 50 μ m. Arrowheads show intercellular gaps that formed after exposure to HP.

TABLE 1. Morphologic parameters of ECs exposed to HP.

	Aspect ratio	Orientation angle (°)	Tortuosity
Static	0.697 ± 0.138	5.016 ± 49.816	1.134 ± 0.059
Control (h)			
3	0.688 ± 0.136	2.744 ± 50.135	1.126 ± 0.052
6	0.690 ± 0.155	4.476 ± 51.458	1.120 ± 0.055
12	0.677 ± 0.132	8.122 ± 49.328	1.132 ± 0.053
24	0.719 ± 0.121	3.309 ± 49.538	1.126 ± 0.052
-50 mmHg (h)			
3	0.702 ± 0.129	2.896 ± 52.265	1.125 ± 0.058
6	0.704 ± 0.137	1.386 ± 52.740	1.133 ± 0.059*
12	0.703 ± 0.123	-1.622 ± 51.417	1.124 ± 0.054
24	0.687 ± 0.135*	2.027 ± 52.538	1.128 ± 0.049
+50 mmHg (h)			
3	0.711 ± 0.138	3.925 ± 50.986	1.119 ± 0.045
6	0.688 ± 0.129	5.150 ± 51.541	1.130 ± 0.055
12	0.695 ± 0.128	0.465 ± 49.227	1.131 ± 0.051
24	0.723 ± 0.116	0.648 ± 50.086	1.118 ± 0.044

Values are mean ± SD. A two-tailed *t* test was used to determine the significance of differences between values (**p* < 0.01).

Mean ± SD, *n* = 3 (300 cells), or *n* = 4 (400 cells) only for +50 mmHg for 24 h.

* *p* < 0.01 vs. Control at the same time point.

were observed between parameters under different conditions, no significant exposure time-related trends were observed. With respect to orientation angle, the SD under the all conditions was over 45°, indicating that the ECs were randomly oriented.

Cell Area and Density

Cell area decreased with increasing exposure time under all conditions examined, as illustrated in Fig. 3. Significant differences were found between the control cells and cells exposed to HP. For the control condition with a 12-h exposure, the average cell area was 1723 + 753 μm² (open bar), whereas the average area of cells exposed to -50 mmHg was only approximately 80% of that value, at 1339 + 590 μm² (hatched bar; mean + SD; ***p* < 0.001).

For 24-h exposure to pressure, the cell area was 80% or less of that of control cells. The area of cells exposed to -50 mmHg was 1214 + 477 μm² (hatched bar; mean + SD; ***p* < 0.001), and the area of cells exposed to +50 mmHg was 946 + 375 μm² (gray closed bar; mean + SD; ***p* < 0.001).

Data regarding cell density (number of cells per 100-μm square) after exposure to HP are presented in Fig. 4. Under negative pressure (-50 mmHg), the density peaked at 12 h of exposure and then decreased until 24 h. In contrast, under positive pressure (+50 mmHg), the cell density increased with exposure time, peaking at 24 h of exposure. The density of cells under the control condition increased linearly and slightly with exposure duration. A significant difference (***p* < 0.001) was noted between the peak density in the control and pressure conditions.

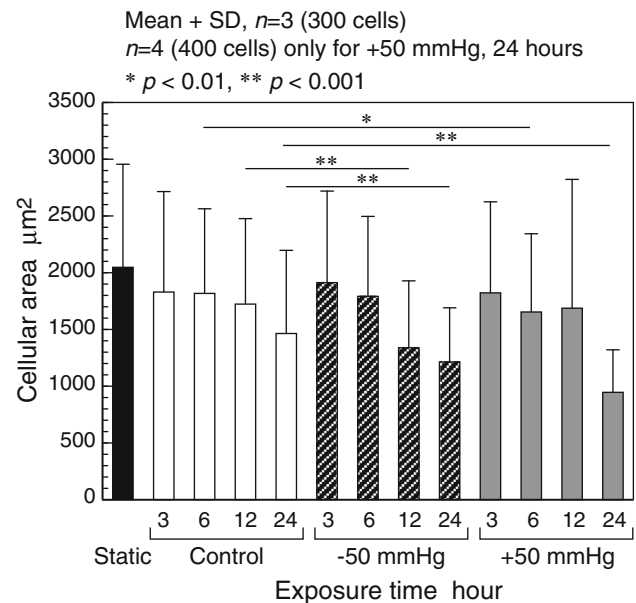


FIGURE 3. Changes in cell area after exposure to HP. Static cultured, control (0 mmHg), negative pressure (-50 mmHg), and positive pressure (+50 mmHg) conditions are indicated by black closed bars, open bars, hatched bars, and gray closed bars, respectively. Values are mean ± SD. A two-tailed *t* test was used to determine the significance of differences between values (p* < 0.01 and ***p* < 0.001).**

Intercellular Gap Formation

Although HUVECs maintained a confluent monolayer under all conditions examined in this study, gaps formed between cells after exposure to HP, as indicated by the white arrowheads in Fig. 2. The gaps could be observed as soon as 3 h before the cell density

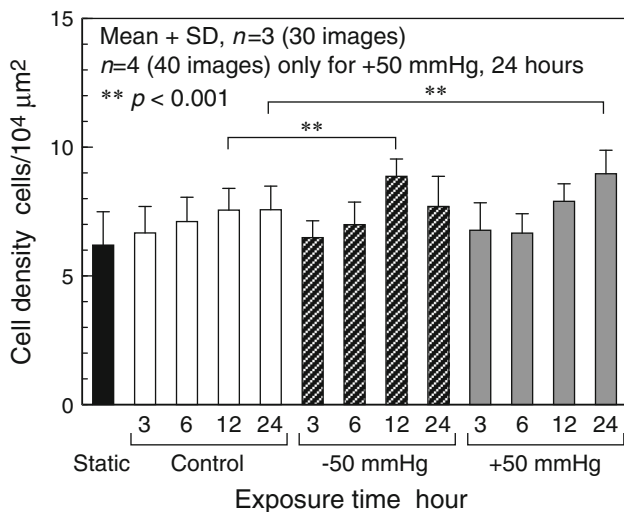


FIGURE 4. Changes in cell density after exposure to HP. Static cultured, control (0 mmHg), negative pressure (-50 mmHg), and positive pressure (+50 mmHg) conditions are indicated by black closed bars, open bars, hatched bars, and gray closed bars, respectively. Values are mean \pm SD. A two-tailed *t* test was used to determine the significance of differences between values (** $p < 0.001$).

peaked. Slight denudation of ECs exposed to HP was also observed after the cell density peaked. In contrast, no formation of intercellular gaps, denudation, or damage were observed under the control condition.

Cell Cycle

Figure 5 shows the percentage of HUVECs existing in S and G2/M phases after exposure to ± 50 mmHg. The percentage of cells in S and G2/M phases was about 20% of the total under static culture, and thus

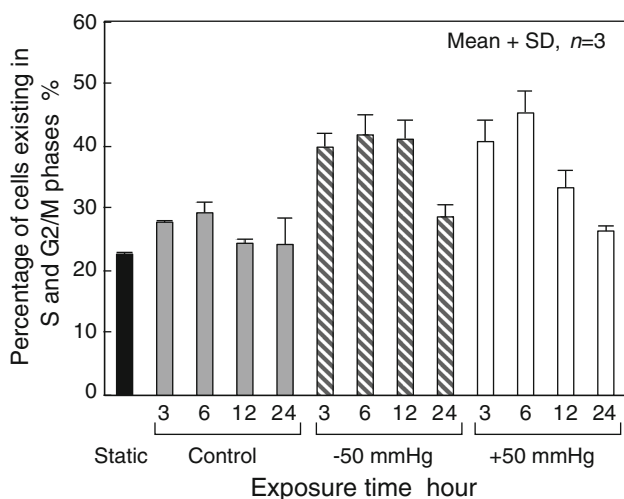


FIGURE 5. Percentage of HUVECs existing in S and G2/M phases after exposure to HP.

most of cells remained in G1 phase. For the control condition, the percentage of the cells in S and G2/M phases had similar value to that under static culture. On the other hand, after exposing ± 50 mmHg, the percentage reached to 40% or more in from 3 to 6 h exposure and then decreased. We confirmed that cell cycle of highly confluent HUVECs, which remained in G1 phase according to contact inhibition, was forcibly progressed by HP.

DISCUSSION

The results of the present study demonstrate that exposure to HP has no significant effect on important morphologic characteristics of cells, as determined from quantitative analyses of the aspect ratio, orientation angle, and tortuosity. However, exposure to HP did induce a decrease in cell area and an increase in cell density with increasing exposure duration. Exposure to HP also progressed of cell cycle, which remained at rest according to contact inhibition of HUVECs. Considering these changes and the observed formation of intercellular gaps, we conclude that exposure to HP enhances the proliferation of ECs. Although there were some differences with respect to trends in changes in cell area and density, positive and negative pressures had similar effects on ECs. The effects of sustained exposure to pressure become less persistent for endothelial function. This notion is supported by the finding that percentage of ECs existing in proliferative phases reached to peak in from 3 to 6 h exposure to HP and then decreased. Consequently, changes in HP may play an important role in EC responses.

Why were there no pressure-induced changes in the morphologic parameters we examined? ECs are known to change their morphology as a result of sensing the direction of mechanical stimuli. Assuming that a cell exhibits isotropic elasticity, HP, which is a surface force, does not generate direction of a force that acts on ECs. Additionally, the internal and external pressures affecting a cell may be continually counterbalanced; as cells are composed primarily of water, the force field within the cell is not affected by a change in HP. Positive or negative pressures on the order of 50 mmHg are not sufficient to alter or damage the structure of intracellular proteins. Several studies have examined the effect of HP on cell morphology. Bovine aortic ECs (BAECs) are known to elongate and increase in tortuosity after 24 h of exposure to +50 mmHg generated through a flow-exposure system.¹⁵ BAECs also reportedly elongate after 24 h of exposure to +100 mmHg with marginal shear flow with 0.1 Pa or less.²⁰ These studies also reported that BAECs exposed to pressure exhibit a multilayered

structure. These results are inconsistent with the results of the present study, however. The systems used in previous studies generate a small spatial gradient of pressure through the combined effect of HP and shear stress, with minimal influence on cell morphology, in contrast to our system. Other researchers have shown that ECs elongate under combined HP and shear stress.¹⁸ It was also reported that multiple mechanical stimuli synergistically influence cell morphology and increase the sensitivity of cells to stimuli.²⁵ Upon exposure to combined mechanical stimuli, the sensitivity of ECs in terms of the ability to detect shear flow may increase. However, even if ECs are exposed to pressure generated without shear flow, they exhibit elongation and a multilayered structure.¹⁷ Most of the studies that have reported multilayering of ECs have used BAECs or bovine pulmonary artery ECs. The formation of a multilayered structure in pressure-exposed ECs may be a species-specific response to HP. In fact, one study showed that HUVECs do not exhibit a multilayered structure in comparison with bovine ECs.¹⁴ HUVECs also tend to align and elongate in parallel to the flow direction after exposure to HP generated using flow exposure systems.¹⁴ As the sensitivity of ECs to shear flow depends on their animal species or type of organ from which they are isolated,⁵ low shear stress may induce morphologic changes in HUVECs. In contrast, another study found no morphologic changes in porcine pulmonary artery ECs and myocardial mouse ECs following exposure to up to +15 cmH₂O without fluid flow.¹² These results agree with our results, which were obtained by subjecting ECs to HP alone.

In the present study, both cell area and cell density changed, intercellular gaps formed, and cell cycle progression were promoted after exposure to HP, even though no changes in morphologic parameters were observed. As no changes in the force field should occur upon the application of HP, why did these phenomena occur? The 50 mmHg of positive and negative HP applied in the present study would not directly affect the force field within a cell but could alter the chemical potential slightly. If the stimulus resulting from such a change in the chemical potential is transmitted through the cell membrane into the cell, the cell could in response dissipate the stimulus by altering its chemical potential through activation of transmembrane channels (e.g., aquaporin water channels) in an isothermal process governed by Le Chatelier's principle.^{2,10} During exposure to HP, entropy also changes in the cell. Actin filaments, which are components of the cytoskeleton, respond to osmotic stress through changes in their chemical potential resulting from their internal energy.¹⁰ Mechanical stress alters the cross-linked structure of actin filaments, and under this stress they exhibit a unique non-linear elastic behavior.¹⁶ Actin

filaments thus exhibit entropic elasticity controlled by entropic change.⁶

In addition to actin filaments, other proteins and DNA may be influenced by entropic change. Changes in entropy or chemical potential caused by exposure to HP may induce the formation of intercellular gaps and enhance cell growth. The formation of intercellular gaps as a result of disassociation of adherens junctions (VE-cadherin) is known to increase activity of Ras homolog gene family, member A (RhoA), which plays an important role in cell proliferation.¹³ Previous studies have indicated that exposure to negative or positive pressure enhances the proliferation and migration of ECs.^{3,19} Positive pressure reportedly results in cell cycle progression¹⁹ and downregulated expression of VE-cadherin¹⁴ in HUVECs. These results agree with the results of the present study.

In conclusion, the results of the present study suggest that changes in HP can enhance cell proliferation without causing morphologic changes in ECs. The enhancement of cell proliferation may be caused by the changes in the chemical potential or entropy depending on not HP value but changes in HP. Thus, ECs responded similarly to both negative and positive pressures. The findings about enhancement of cell proliferation are conducive to promotion of angiogenesis in the pressure treatment. However, the mechanisms by which ECs respond to stimuli caused by changes in entropy or chemical potential after exposure to HP have yet to be elucidated and will be investigated in future studies. In addition, it is necessary to study effects of HP on other kinds of cell such as epithelial cells or fibroblasts, which exist in wound environment, for developing the pressure treatment.

CONFLICT OF INTEREST

D.Y., K.S., and M.S. declare that they have no conflict of interest.

ETHICAL STANDARDS

No human studies were carried out by the authors for this article. No animal studies were carried out by the authors for this article.

REFERENCES

- ¹Argenta, L. C., and M. J. Morykwas. Vacuum-assisted closure: a new method for wound control and treatment: clinical experience. *Ann. Plast. Surg.* 38:563–576, 1997.
- ²Atkins, P., and J. de Paula. *Atkins' Physical Chemistry* (8th ed.). Oxford: Oxford University Press, 2006.

- ³Baldwin, C., M. Potter, E. Clayton, L. Irvine, and J. Dye. Topical negative pressure stimulates endothelial migration and proliferation: a suggested mechanism for improved integration of Integra. *Ann. Plast. Surg.* 62:92–96, 2009.
- ⁴DeFranzo, A. J., L. C. Argenta, M. W. Marks, J. A. Molnar, L. R. David, L. X. Webb, W. G. Ward, and R. G. Teasdall. The use of vacuum-assisted closure therapy for the treatment of lower-extremity wounds with exposed bone. *Plast. Reconstr. Surg.* 108:1184–1191, 2001.
- ⁵Fisher, A. B., S. Chien, I. A. Barakat, and R. M. Nerem. Endothelial cellular response to altered shear stress. *Am. J. Lung Cell Mol. Physiol.* 281:529–533, 2001.
- ⁶Gardel, M. L., J. H. Shin, F. C. MacKintosh, L. Mahadevan, P. Matsudaira, and D. A. Weitz. Elastic behavior of cross-linked and bundled actin networks. *Science* 304:1301–1305, 2004.
- ⁷Genecov, D. G., A. M. Schneider, M. J. Morykwas, D. Parker, W. L. White, and L. C. Argenta. A controlled subatmospheric pressure dressing increases the rate of skin graft donor site reepithelialization. *Ann. Plast. Surg.* 40:219–225, 1998.
- ⁸Hothorn, T., and B. S. Everitt. *A Handbook of Statistical Analyses Using R* (3rd ed.). Boca Raton: Chapman & Hall/CRC, 2014.
- ⁹Hsu, C. C., W. C. Tsai, C. P. Chen, Y. M. Lu, and J. S. Wang. Effects of negative pressures on epithelial tight junctions and migration in wound healing. *Am. J. Physiol. Cell Physiol.* 299:C528–C534, 2010.
- ¹⁰Ito, T., and M. Yamazaki. The “Le Chatelier’s principle”-governed response of actin filaments to osmotic stress. *J. Phys. Chem. B* 110:13572–13581, 2006.
- ¹¹Lambert, K. V., P. Hayes, and M. McCarthy. Vacuum assisted closure: a review of development and current applications. *Eur. J. Vasc. Endovasc. Surg.* 29:219–226, 2005.
- ¹²Müller-Marschhausen, K., J. Waschke, and D. Drenckhahn. Physiological hydrostatic pressure protects endothelial monolayer integrity. *Am. J. Physiol. Cell Physiol.* 294:C324–C332, 2008.
- ¹³Noren, N. K., C. M. Niessen, B. M. Gumbiner, and K. Burridge. Cadherin engagement regulates Rho family GTPases. *J. Biol. Chem.* 276:33305–33308, 2001.
- ¹⁴Ohashi, T., K. Segawa, N. Sakamoto, and M. Sato. Effect of hydrostatic pressure on the morphology and expression of VE-cadherin in HUVEC. *Trans. Jpn. Soc. Med. Biol. Eng. BME* 44:454–459, 2006.
- ¹⁵Ohashi, T., Y. Sugaya, N. Sakamoto, and M. Sato. Hydrostatic pressure influences morphology and expression of VE-cadherin of vascular endothelial cells. *J. Biomech.* 40:2399–2405, 2007.
- ¹⁶Pujol, T., O. du Roure, M. Fermigier, and J. Heuvingh. Impact of branching on the elasticity of actin networks. *Proc. Natl. Acad. Sci. USA* 109:10364–10369, 2012.
- ¹⁷Salwen, S. A., D. H. Szarowski, J. N. Turner, and R. Bizios. Three-dimensional changes of the cytoskeleton of vascular endothelial cells exposed to sustained hydrostatic pressure. *Med. Biol. Eng. Comput.* 36:520–527, 1998.
- ¹⁸Sato, M., and T. Ohashi. Biorheological views of endothelial cell responses to mechanical stimuli. *Biorheology* 42:421–441, 2005.
- ¹⁹Schwartz, E. A., R. Bizios, M. S. Medow, and M. E. Gerritsen. Exposure of human vascular endothelial cells to sustained hydrostatic pressure stimulates proliferation. Involvement of the α V integrins. *Circ. Res.* 84:315–322, 1999.
- ²⁰Sugaya, Y., N. Sakamoto, T. Ohashi, and M. Sato. Elongation and random orientation of bovine endothelial cells in response to hydrostatic pressure: comparison with response to shear stress. *JSME Int. J.* 45:1248–1255, 2003.
- ²¹Sullivan, N., D. L. Snyder, K. Tipton, S. Uhl, and K. M. Schoelles. Negative pressure wound therapy devices (Project ID: WNDT1108). Technology Assessment Report, AHRQ USA. (Available online 26 May 2009).
- ²²Ubbink, D. T., S. J. Westerbos, D. Evans, L. Land, and H. Vermeulen. Topical negative pressure for treating chronic wounds. *Cochrane Database Syst. Rev.* 16:CD001898, 2008.
- ²³Ubbink, D. T., S. J. Westerbos, E. A. Nelson, and H. Vermeulen. A systematic review of topical negative pressure therapy for acute and chronic wounds. *Br. J. Surg.* 95:685–692, 2008.
- ²⁴Velnar, T., T. Bailey, and V. Smrkolj. The wound healing process: an overview of the cellular and molecular mechanisms. *J. Int. Med. Res.* 37:1528–1542, 2009.
- ²⁵Zhao, S., A. Suciu, T. Ziegler, J. E. Moore, Jr., E. Bürki, J. J. Meister, and H. R. Brunner. Synergistic effects of fluid shear stress and cyclic circumferential stretch on vascular endothelial cell morphology and cytoskeleton. *Arterioscler. Thromb. Vasc. Biol.* 15:1781–1786, 1995.